Supporting Information

First evaluation of multifunctional poly(ionic liquid)s as novel strong bases in directional efficient valorization of lignin

Guoqiang Zhang, Zhongqiu Liu*, Yinuo Li, Yuanyuan Yu, Yujing Liu, Anguo Ying*

Key Laboratory of Life-Organic Analysis of Shandong Province, School of Chemistry and Chemical Engineering, Qufu Normal University, Qufu 273165, Shandong, P.R. China

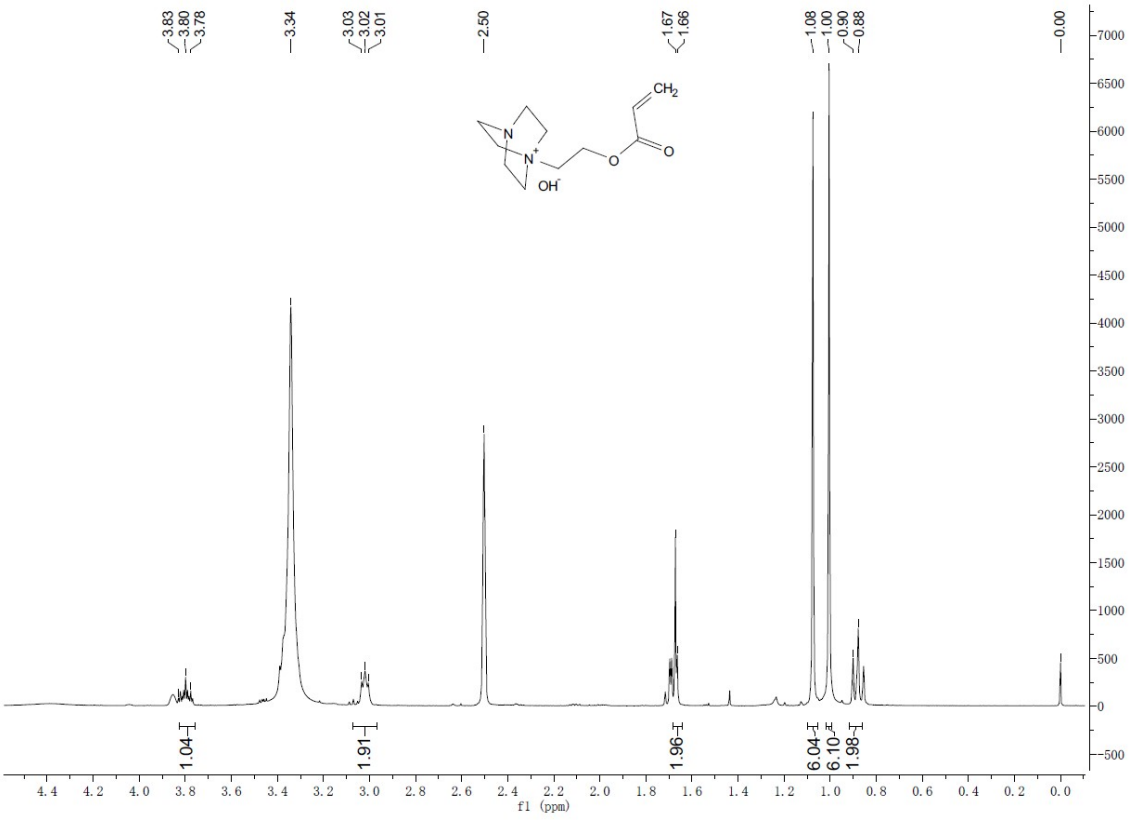

Fig. S1 1-(2-(acryloyloxy)ethyl)-4-aza-1-azoniabicyclo[2.2.2]octane hydroxide. ^{1}H NMR (500 MHz, DMSO-d6) δ 3.80 (ddd, J = 11.3, 7.2, 4.1 Hz, 1H), 3.03 (m, 2H), 1.68 (m, 2H), 1.08 (s, 6H), 1.00 (s, 6H), 0.88 (m, 2H).

* Corresponding author. Tel: +86 537 4458301, Fax: +86 537 4458301.
E-mail address: liuzhongqiuzs@126.com (Z. Liu); yinganguo@163.com (A. Ying).

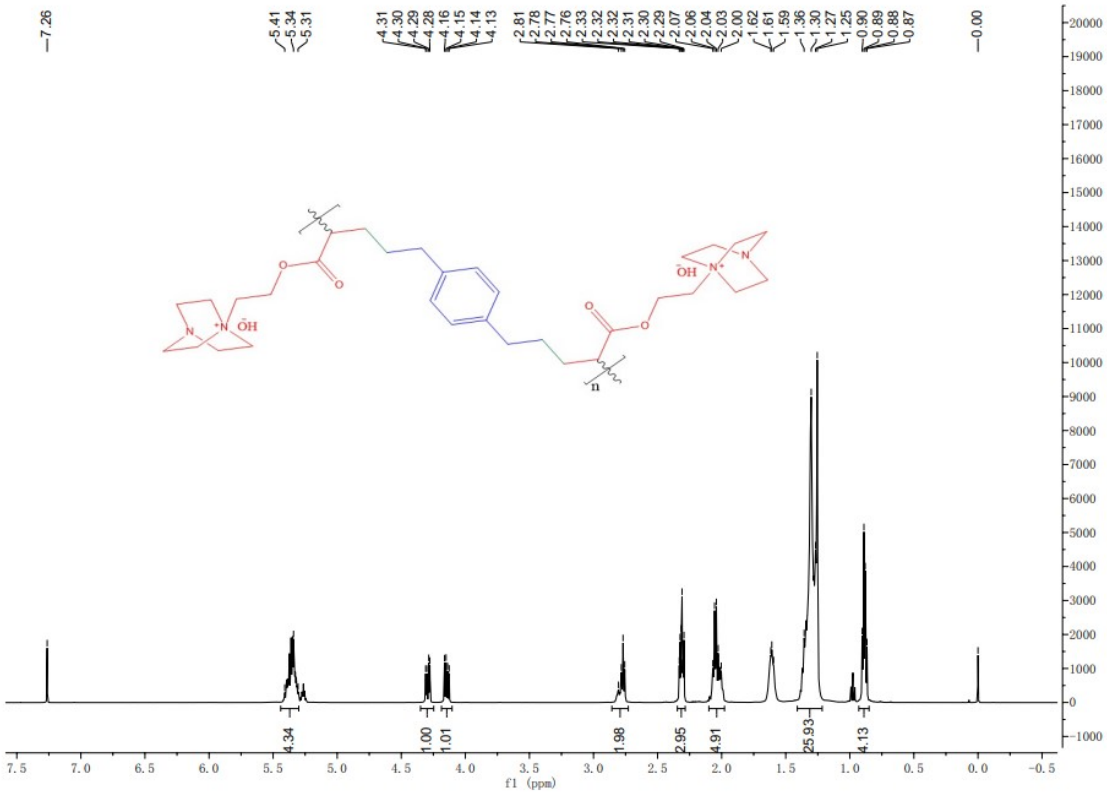

Fig. S2 P(3DVB-[AD][OH]) in absence of Fe_3O_4 nanoparticles. ^{1}H NMR (500 MHz, Chloroform-*d*) δ 5.44 – 5.30 (m, 4H), 4.14 (dd, *J* = 11.9, 6.0 Hz, 1H), 2.86 – 2.73 (m, 2H), 2.31 (td, *J* = 7.6, 3.3 Hz, 3H), 2.05 (h, *J* = 6.0, 5.4 Hz, 5H), 1.41 – 1.22 (m, 26H), 0.88 (td, *J* = 6.9, 4.7 Hz, 4H).

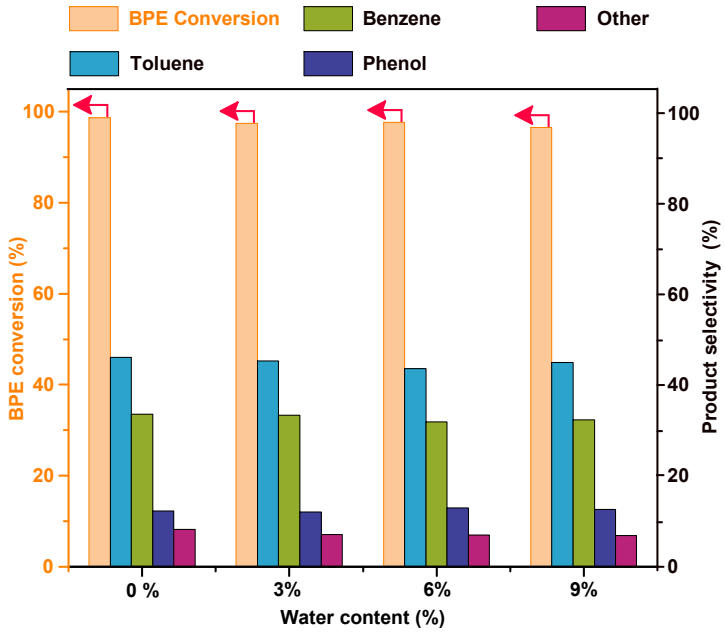

Fig. S3 BPE conversion and product selectivity in mixed solvents of *h*-hexane and H_2O. Reaction conditions: 1.0 mmol BPE, 0.10 g P(3DVB-[AD][OH]), 300 ℃, 8 h, and 20 mL solvent (*h*-hexane:H_2O=100:0, *h*-hexane:H_2O=97:3, *h*-hexane:H_2O=94:6 and *h*-hexane:H_2O=91:9).

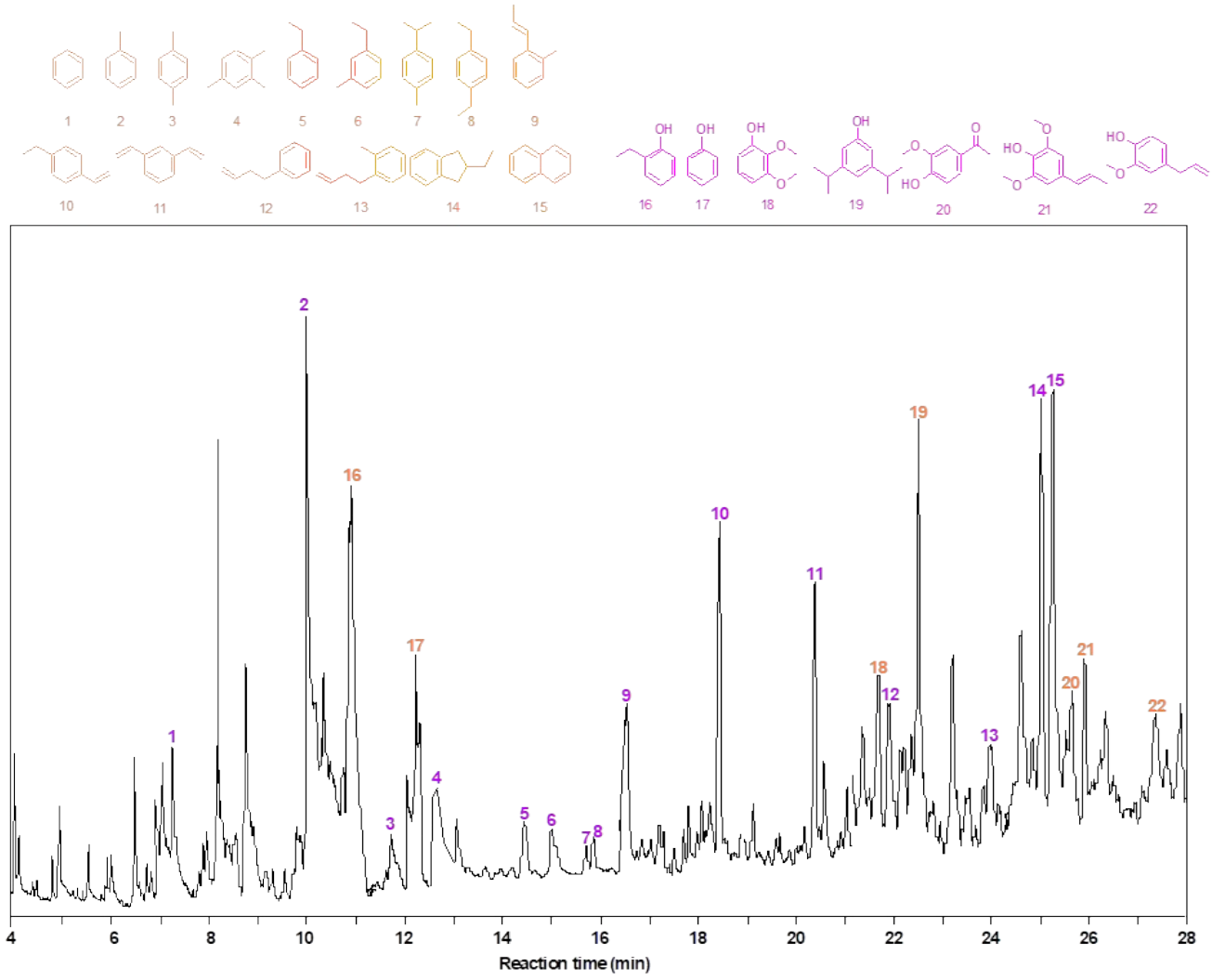

Fig. S4 Total ion chromatogram of catalytic hydroconversion of lignin over P(3DVB-[AD][OH]).

To gain further insight into the outstanding catalytic properties of poly(ionic liquid)s, the XPS characterization was conducted on fresh Kraft lignin and its depolymerized residue. According to **Fig. S5**, there are mainly three types of carbon species existed in fresh Kraft lignin. The binding energy located at 284.98 eV (C_{2a}) can be attributed to C–OH and the binding energy located at 288.48 (C_4) and 292.98 eV (C_5) is generally in line with O=C–O and transitions in π-electrons of aromatic rings (shake up-satellite), respectively.[S1,S2] Compared with the residue sample, the peak position of C_{2a}, C_4, and C_5 markedly shifts to a lower binding energy, which is ascribed to the directional cleavage of the C–O

bonds. In addition, the binding energy located at 285.78 eV (C_{2b}) can be attributed to C–OR, suggesting MFPILs efficiently promote the cleavage of C–O bond to various MCACs. The ratio between C_4 and C_5 in fresh Kraft lignin is remarkably higher than those in residue. The typical band of deformation vibrations of C–H bonds in syringyl rings and C–O stretch in alcohols /or ethers is near 1122 and 1196 cm^{-1} in IR spectrum, respectively, and these peaks ever existed in the lignin but diminished significantly in the solid residue after catalytic depolymerization. These results clearly illustrate that P(3DVB-[AD][OH]) plays a very significant role in the catalytic cleavage of C–O bridged bonds connecting some arene rings in lignin.

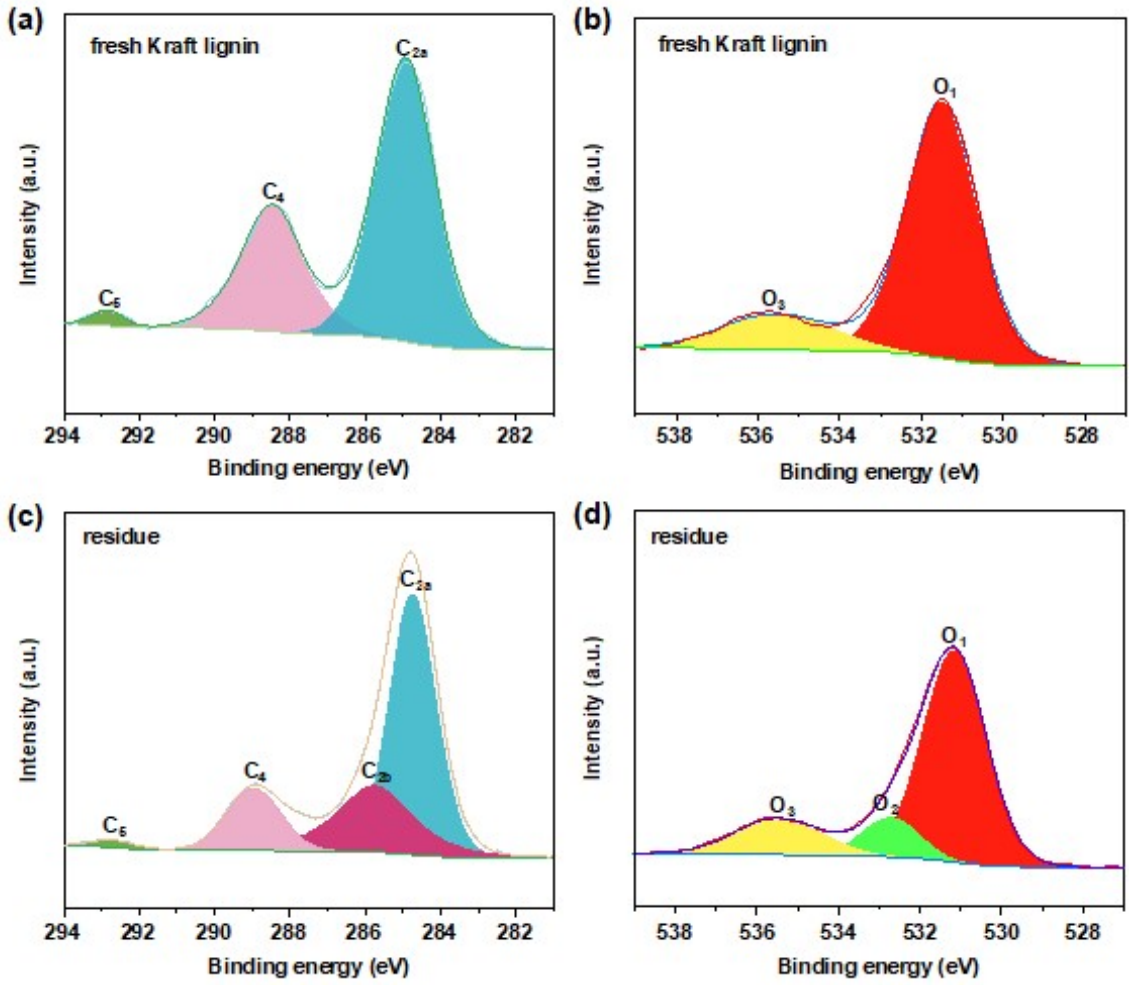

Fig. S5. XPS spectra of fresh Kraft lignin and residue.

Subsequently, the lignin O1s spectrum was studied in **Fig. S5**, it was discovered that there were three kinds of oxygen signal peaks appeared in the residue. The peak located at 532.68 eV (O_2) can be attributed to C–OH, C=O, and O–C=O and the peak observed at 531.48 (O_1) can be assigned to benzyl aryl ether and diary ether. In addition, the peak located at 535.98 eV (O_3) can be assigned to phenolic-OH, aliphatic aromatic ether, and acids.[S3] Compare with fresh Kraft lignin, the ratio of O_1 and O_3 in residue becomes weaker. Also, the signal peak of O1s shifts to a lower binding energy, indicating that MFPILs efficiently facilitate the cleavage of aromatic ether in lignin. These evidences further demonstrate that MFPILs have a significant influence on C–O band dissociation in lignin.

As shown in **Fig. S6**, all the peaks appearing in the fresh Kraft lignin sample are also retained in the residue but their intensity changed, indicating that the overall structure of lignin (and substituents) is changed after depolymerization. The peak in 14.4 ppm is typically assigned to γ−CH_3 in n-propyl side chain. The observance of peaks in range of 27−30 ppm is assigned to −CH_2− in aliphatic side chain and 30-36.8 is corresponded to −CH_3 group in aliphatic chain, and their intensities are elevated in residue in comparison to fresh Kraft lignin, which may be a result of lignin degradation or cleavage of the side chains in fresh Kraft lignin during the catalytic reaction. At the same time, it is also seen that there is peak at 55.6 ppm assigned to −OCH_3, where is decreased in compared with the fresh one. In the case of residue, the appearance of peak at 60.2 ppm assigned to C-γ in G type β-O-4 units is decreased. Following, the peaks at 100–115, 115–140, and 145-150 ppm belonged to the aromatic regions of lignin are reduced. Of these the peaks at 100–115 and 115–140 ppm is assigned to the C2, C5 of G, C2, C6 of S units and etherified C-1 of G and S units, C-3/C-5 in *p*-hydroxyphenyl, C-6 in G units. Thus,

the peak at 145 ppm belongs to no etherified C-4 in G units.[S6] Lastly, the signals near 170 ppm is mostly associated with carboxyl and a distinct signal at 178 ppm is mostly due to carbonyl.[S7] Interestingly, it can be seen that the peak intensity in residue is moderately decreased, implying that during depolymerization of lignin these bonds are broken, followed by giving the desired products.

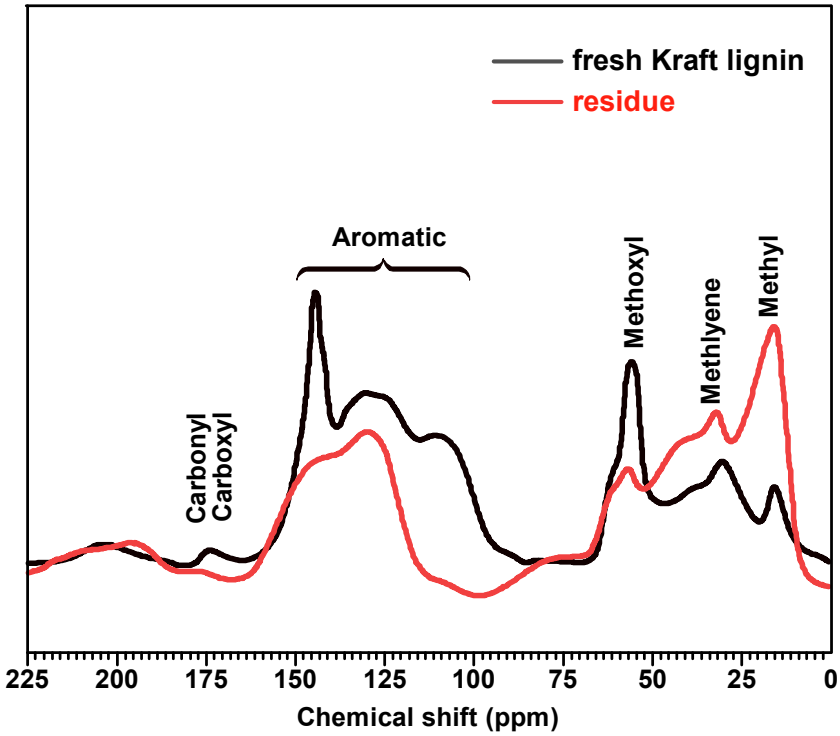

Fig. S6. Solid-state ^{13}C NMR spectrum of fresh Kraft lignin and its catalytic residue.

To further investigate the effects of the MFPILs catalysts on the change of chemical and structural transformations in these samples during the catalytic depolymerization, ^{31}P NMR characterization technique was conducted on the phosphitylated fresh Kraft lignin and its catalytic residue. The information of substructures could be obtained by assigning the signals according to the previous publications.[S8] As shown in **Fig. S7**, the peak intensity of aliphatic OHs decreased significantly from fresh Kraft to residue sample, suggesting that there is remarkably side chain hydroxyl group left in the catalytic depolymerization process. More importantly, the peak intensity of S-type phenolic OH groups

were greatly decreased, while peak of G-and *p*-hydroxyphenyl OH were obviously increased, indicating the S-type units were more susceptible to demethoxylation than G-type units. In addition, the content of carboxylic groups in residue sample is decreased compared with the fresh Kraft lignin, which is probably attributable to the cleavage of lignin. This is in good agreement with the results of solid-state ^{13}C-NMR.

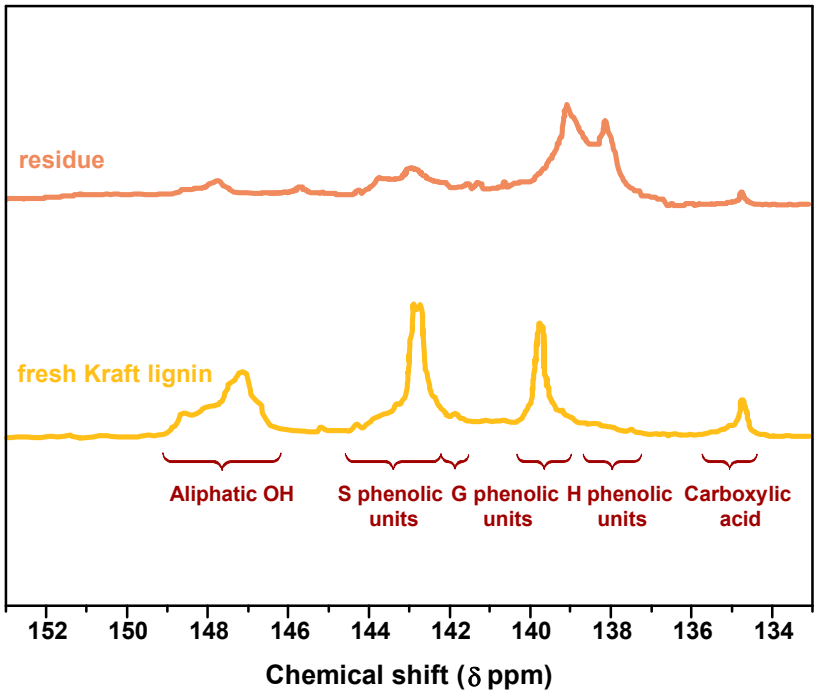

Fig. S7. ^{31}P NMR spectra of fresh Kraft lignin and its catalytic residue after phosphitylation.

Table S1 The molar ratio of starting materials in the preparation process of MFPILs.

Entry	The molar ratio of DVB/[AD][OH]	DVB (mmol)	[AD][OH] (mmol)	vinyl-modified Fe_3O_4 nanoparticles (mg)
1	0.5:1	0.5 mmol	1 mmol	200 mg
2	1:1	1 mmol	1 mmol	200 mg
3	2:1	2 mmol	1 mmol	200 mg
4	3:1	3 mmol	1 mmol	200 mg
5	4:1	4 mmol	1 mmol	200 mg
6	5:1	5 mmol	1 mmol	200 mg
7 [a]	4:1	4 mmol	1 mmol	0 mg

[a]: P(3DVB-[AD][OH]) in absence of Fe_3O_4 nanoparticles.

Table S2 Comparsion of the depolymerization reaction of lignin in different catalyst system.

Entry	Feedstock	Catalyst	Reaction condition	Monomer yield (wt.%)	Ref.
1	Organolsolv lignin	NaOH	300 °C, 90 MPa IHP, 40 min	15.79	1
2	Organocell lignin	Fe_2O_3	380 °C, 10 MPa IHP, 67 min	<17.00	2
3	Hydrolysis lignin	NiMoP/γ-Al_2O_3	380 °C ,7 MPa IHP, 60 min	<10.00	3
4	Maf lignin	NiMo	400 °C, 10 MPa IHP, 20 min	3.80	4
5	Organosolv lignin	Ni/Si-Al_2O_3	390 °C, 1 MPa IHP, 30 min	5.00	5
6	Kraft lignin	Mo_2C/CNF	300 °C, 5 MPa IHP, 4 h	6.00	6

Table S3 The distributions of arenes.

arenes	yield (wt.%)
benzene	0.64
toluene	4.62
p-xylene	1.49
1,2,4-trimethylbenzene	1.13
ethylbenzene	0.48
1-ethyl-3-methylbenzene	0.59
p-cymene	0.38
1,4-diethylbenzene	0.29
(*E*)-1-methyl-2-(prop-1-en-yl)benzene	1.40
1-ethyl-4-vinylbenzene	1.36
1,3-divinylbenzene	0.89
but-3-en-1-ylbenzene	0.33
1-(but-3-en-1-yl)-2-methylbenzene	0.30
2-ethyl-2,3-dihydro-1*H*-indene	0.43
naphthalene	0.56
other arenes	0.50
total	15.39

Table S4 The distributions of arenols.

arenols	yield (wt.%)
phenol	1.24
2-ethylphenol	3.16
2,3-dimethoxyphenol	0.36
3,5-diisopropylphenol	0.53
1-(4-hydroxy-3-methoxyphenyl)ethan-1-one	0.27
(*E*)-2,6-dimethoxy-4-(prop-1-en-1-yl)phenol	0.18
4-allyl-2-methoxyphenol	0.62
other arenols	0.24
total	6.60

Table S5 The distributions of other products

other products	yield (wt.%)
aldehydes	4.37
esters	3.41
alcohols	4.43
other	7.04
total	19.25

(**Table S3-S5)** Yields of GC-MS detectable SPs obtained by catalytic hydrogenolysis of lignin using P(3DVB-[AD][OH]). Reaction conditions: catalyst 0.1 g, lignin 0.1 g, *n*-hexane 20 mL, 300 ^{o}C, 5 MPa IHP, for 8 h.

Table S6 The lignin conversion and yields of SPs over P(3DVB-[AD][OH])[a] and P(3DVB-[AD][OH])

catalysts	**lignin conversion (%)**	**yield (wt.%)**					
		arenes	arenols	aldehydes	esters	alcohols	other
P(3DVB-[AD][OH]) [a]	24.68	6.18	2.46	2. 69	2.70	2.95	7.70
P(3DVB-[AD][OH])	41.24	15.39	6.60	4.37	3.41	4.43	7.04

Reaction conditions: catalyst 0.1 g, lignin 0.1 g, *n*-hexane 20 mL, 300 ^{o}C, 5 MPa IHP, and 8 h.

[a]: P(3DVB-[AD][OH]) in absence of Fe_3O_4.

Table S7 The XPS results for fresh Kraft lignin and residue.

Peaks	Sample	Fresh Kraft lignin	Residue
C_{1s}	C_{2a} (eV)	284.98	284.78
	C_{2a} (area%)	66.9	57.34
	C_{2b} (eV)	-	285.78
	C_{2b} (area%)	-	25.94
	C_4 (eV)	288.48	288.98
	C_4 (area%)	32.0	15.2
	C_5 (eV)	292.98	292.78
	C_5 (area%)	11.1	1.52
O_{1s}	O_1 (eV)	531.48	531.28
	O_1 (area%)	82.5	71.1
	O_2 (eV)	-	532.68
	O_2 (area%)	-	12.0
	O_3 (eV)	535.58	535.98
	O_3 (area%)	17.5	16.9

References:

S1 J. Laine, P. Stenius, G. Carlsson and G. Ström, *Cellulose*, 1994, **1,** 145-160.

S2 J. B. Guo, Z. Y. Tao and X. G. Luo, *Acta Chimica Sinica*, 2005, **63**, 1536-1540.

S3 A. Ahmed, A. Adnot and S. Kaliaguine, J. App. Polym. Sci., 1987, 34, 359-375.

S4 S. N. Sun, M. F. Li, T. Q. Yuan, F. Xu and R. C. Sun, Ind. Crop. Prod., 2012, 37, 51-60.

S5 M. S. Jahan, D. A. N. Chowdhury, M. K. Islam and S. M. I. Moeiz, Bioresource Technol., 2007, 98, 465-469.

S6 J. L. Wen, S. L. Sun, B. L. Xue, and R. C. Sun, Materials, 2013, 6, 359-391.

S7 D. F. Cipriano, L. S. Chinelatto Jr, S. A. Nascimento, C. A. Rezende, S. M. C. de Menezes And J. C. C. Freitas, Biomass & Bioenergy, 2020, 142, 105792.

S8 T. Parsell, S. Yohe, J. Degenstein, T. Jarrell, I. Klein, E. Gencer, B. Hewetson, M. Hurt, J.I. Kim, H. Choudhari, B. Saha, R. Meilan, N. Mosier, F. Ribeiro, W.N. Delgass, C. Chapple, H.I. Kenttamaa, R. Agrawal and M.M. Abu-Omar, Green Chem., 2015, 17, 1492-1499.